JOURNAL OF SOLID STATE CHEMISTRY 77, 162–169 (1988)

Preparation, Crystal Structure, and Luminescence of Magnesium Molybdate and Tungstate Monohydrates, $MgMoO_4 \cdot H_2O$ and $MgWO_4 \cdot H_2O$

M. AMBERG, J. R. GÜNTER,[1] AND H. SCHMALLE

Institute for Inorganic Chemistry, University of Zürich, Winterthurerstrasse 190, CH-8057 Zürich, Switzerland

AND G. BLASSE

Physical Laboratory, University of Utrecht, P.O. Box 80.000, 3508 TA Utrecht, The Netherlands

Received April 14, 1988; in revised form July 7, 1988

Triclinic $MgMoO_4 \cdot H_2O$ and the isomorphous $MgWO_4 \cdot H_2O$ have been prepared under mild hydrothermal conditions in single crystalline form and the crystal structure of $MgMoO_4 \cdot H_2O$ has been determined by X-ray diffraction. The structure is compared to a model deduced earlier for $MgWO_4 \cdot H_2O$ from topotaxy data, with which the general topology agrees, but there is an important difference in the orientation of MoO_4-tetrahedra. The X-ray powder diffraction data, thermal dehydration behavior, as well as the luminescence properties are reported and the latter compared with data of related phases. Crystal data are: Triclinic, space group $P\,\bar{1}$; $MgMoO_4 \cdot H_2O$: $a = 5.665$ Å, $b = 5.869$ Å, $c = 6.875$ Å, $\alpha = 100.80°$, $\beta = 95.05°$, $\gamma = 106.57°$; $MgWO_4 \cdot H_2O$: $a = 5.681$ Å, $b = 5.887$ Å, $c = 6.870$ Å, $\alpha = 100.85°$, $\beta = 95.44°$, $\gamma = 106.55°$.

Introduction

In an earlier paper (*1*), we have described the crystal structure of magnesium tungstate dihydrate, $MgWO_4 \cdot 2H_2O$, and from a study of the topotaxy of its dehydration, a model for the crystal structure of the monohydrate, $MgWO_4 \cdot H_2O$, has been deduced. We have now succeeded in preparing the monohydrate directly in crystalline form by hydrothermal synthesis under mild conditions, as well as the isomorphous magnesium molybdate monohydrate, $MgMoO_4 \cdot H_2O$, and have determined the crystal structure of the latter from single crystal X-ray diffraction data (*2*). The present paper compares this structure with the model suggested in (*1*), pointing out a difference in the orientation of MoO_4-tetrahedra, and describes the dehydration behavior of the two compounds, as well as their luminescence properties, which are compared to those of related phases. The data presented help in understanding the structural chemistry of magnesium molybdates and tungstates as a family of related compounds.

Preparation of Samples

(a) $MgWO_4 \cdot H_2O$: Equal volumes of 0.75 *M* solutions of Na_2WO_4 and $Mg(NO_3)_2$ in

[1] To whom correspondence should be addressed.

0022-4596/88 $3.00

water are mixed at room temperature and filled into Pyrex tubes to approximately two-thirds of their volume. The closed tubes are put in upright position into an oven and kept at 155°C for 3 days. The crystalline product is filtered, washed with water and ethanol, and dried in air at 90°C.

(b) $MgMoO_4 \cdot H_2O$: Equal volumes of 1 *M* solutions of Na_2MoO_4 and $MgCl_2$ in 0.5 *M* HCl are mixed at room temperature (pH = 6) and filled into Pyrex tubes to approximately two-thirds of their volume. The closed tubes are put in upright position into an oven and kept at 155°C for 3 days. The crystalline product is filtered, washed with water and ethanol, and dried in air at 90°C.

X-ray Powder Diffraction

Whereas the magnesium tungstate monohydrate prepared by dehydration of the dihydrate was of a relatively low degree of crystallinity and heavily twinned, as reported in (*1*), the materials prepared according to the above procedures are much more crystalline, and therefore yield diffraction patterns with more and better resolved lines (Guinier-De Wolff camera, Cu$K\alpha_1$). Following the single crystal experiments (see below), these could be indexed by means of a triclinic unit cell which is four times smaller than the pseudo-monoclinic cell proposed in (*1*). (Lattice constants were calculated by least-squares refinement of powder data; see Table I. Intensities were measured photometrically.) The true symmetry was hidden in the dehydrated samples due to the intense twinning, which hindered a recognition of the systematic absences. The pseudomonoclinic and the triclinic cells are related as follows:

$$a_{tric} = 0.5a_{mono} + 0.25b_{mono} + 0.25c_{mono},$$

$$b_{tric} = -0.5a_{mono} + 0.25b_{mono} + 0.25c_{mono},$$

$$c_{tric} = -0.5b_{mono} + 0.5c_{mono}.$$

TABLE I

X-RAY POWDER DIFFRACTION PATTERNS OF $MgMoO_4 \cdot H_2O$ AND $MgWO_4 \cdot H_2O$

$MgMoO_4 \cdot H_2O$		$MgWO_4 \cdot H_2O$			
d(Å)	I/I_0	d(Å)	I/I_0	$h\ k\ l_{tric}$	$h\ k\ l_{mono}$
6.648	12	6.618	5	0 0 1	0 1 1
5.472	52	5.477	51	0 1 0	−1 1 1
5.349	11	5.386	6	1 0 0	
4.783	17	4.787	30	0 1−1	−1 2 0
4.610	65	4.614	58	1−1 0	2 0 0
4.529	54	4.543	62	1 0−1	1 2 0
3.899	65	3.893	78	1−1 1	1 0 2
3.833	20	3.831	17	0 1 1	−2 1 1
3.691	27	3.701	28	1−1−1	2 1 1
3.350	80	3.357	50	1 1 0	0 2 2
3.331	100	3.329	100	0 0 2	0 3 1
3.313	80			1 1−1	
3.179	49	3.181	35	0 1−2	−1 2 2
2.815	55	2.826	47	1−2 0	−3 1 1
2.780	22	2.777	55	1−1 2	3 1 1
2.770	61			2−1 0	
2.768	65	2.769	47	0 2−1	
2.753	41	2.750	25	1 1 1/0 2 0	0 1 3/−2 2 2
2.695	40	2.705	22	1 1−2	0 4 0
2.681	45	2.688	34	2 0 0	231/−113/113
2.629	23	2.636	11	1−1−2	
2.605	16	2.602	16	0 1 2	
2.598	14	2.608	12	2−1−1	−1 4 0
2.520	7	2.519	9	2−1 1	0 2 3
2.465	4			1−2−1	
2.395	11	2.402	3	0 2−2	
2.371	8			2 0 1	
2.359	18	2.359	18	0 2 1	−2 4 0
2.334	23	2.334	15	1−2 2	2 1 3
2.306	7			2−2 0	
2.263	13	2.275	13	2 0−2	0 4 2
2.241	11	2.243	10	0 1−3	
2.226	26	2.221	13	0 0 3	0 3 3
2.194	28	2.204	14	2 1−1	−1 3 3
		2.187	12	1 2 0/2−1−2	
2.177	9	2.177	9	1 0−3	
		2.166	5	2 1 0	
2.142	11	2.149	10	2−2−1	0 0 4
2.135	8	2.128	6	1 1 2	
2.089	29	2.095	11	1 1−3	0 5 1
		2.085	12	2−1 2	
2.068	28	2.076	14	1 2−2	−3 4 0
2.052	5	2.047	4	1−1 3	
2.017	18	2.026	8	2 1−2	1 5 1
2.011	22	2.013	15	1−2−2	

Note. $MgMoO_4 \cdot H_2O$: $a = 5.665$ Å, $b = 5.869$ Å, $c = 6.875$ Å, $\alpha = 100.80°$, $\beta = 95.05°$, $\gamma = 106.57°$; $MgWO_4 \cdot H_2O$: $a = 5.681$ Å, $b = 5.887$ Å, $c = 6.870$ Å, $\alpha = 100.85°$, $\beta = 95.44°$, $\gamma = 106.55°$.

The indexed powder diffraction patterns for both $MgWO_4 \cdot H_2O$ and $MgMoO_4 \cdot H_2O$ are listed in Table I and compared to the former monoclinic indexing. Table I clearly shows that the two patterns are virtually identical.

Very similar patterns are also observed for pink $CoMoO_4 \cdot H_2O$ and $MnMoO_4 \cdot H_2O$ powders prepared by heating the metal powders with MoO_3 in aqueous suspensions and crystallizing the resulting solutions (*3*).

Crystal Structure Determination

A transparent single crystal of $MgMoO_4 \cdot H_2O$ with approximate dimensions 0.08 × 0.10 × 0.17 mm^3 was used for the collection of intensity data on an Enraf-Nonius CAD-4 diffractometer. Lattice parameters of the triclinic cell (space group $P\,-1$) and crystal orientation were obtained from the least-squares refinement of the Θ angles of 24 reflections in the range $13.3 \leq \Theta \leq 19.9°$: a = 5.662(2) Å, b = 5.861(1) Å, c = 6.869(1) Å, α = 100.84(2)°, β = 95.03(2)°, γ = 106.57(2)°, V = 212.2 $Å^3$, Z = 2, d_{calc} = 3.165 g/cm^3, μ = 28.47 cm^{-1}. The 4429 intensity data (including standards) were collected in the range $1° < \Theta < 37°$ using graphite monochromated Mo$K\alpha$ radiation (h: −9 to +9, k: −9 to +9, l: −11 to +11); variable scan speed between 2.2 and 10.0° min^{-1}. Five standard reflections were remeasured every 3 hr and showed no loss of intensities. The intensity data were reduced to F_{obs} by correcting for Lorentz and polarization effects, 2152 unique reflections remained after averaging 4304 data, R_{int} = 0.016. A numerical absorption correction was carried out using the crystal faces (001), (00 − 1), (010), (0 − 10), (1 − 10), and (− 110) with SHELX76 (*4*). The minimum and maximum transmission coefficients were 0.6748 and 0.7814.

The structure was solved with SHELXS86 (*5*). The 2001 reflections with $I \geq 3\sigma(I)$ were used for the refinement with SHELX76, and reflections −110 and 002 were omitted in the last refinement cycles because secondary extinction was suspected. The hydrogen atoms could be localized in the difference Fourier map, their positional and isotropic temperature parameters being fixed.

Anistropic temperature coefficients were refined for Mg, Mo, and O atoms with a full-matrix least-squares method. Final values of R and R_w are 0.022 and 0.029, based on F_{hkl} including 1999 observed reflections and 64 variables. The function minimized was $\Sigma w(|F_o| - |F_c|)^2$ with $w = 1/\sigma^2(F)$. $(\Delta/\sigma)_{max}$ was 0.002 and in the last refinement cycle. The final difference Fourier map showed 0.74 e $Å^{-3}$ and −1.48 e $Å^{-3}$ max and min electron densities. Positional and isotropic thermal parameters are given in Table II. Interatomic distances and angles are listed in Table III.

Further details relating to the crystal structure determination can be obtained from "Fachinformationszentrum Energie, Physik, Mathematik GmbH, D-7514 Eggenstein-Leopoldshafen 2, Federal Republic of Germany," indicating deposit Number CSD-53035, authors names, and journal reference.

Description of Crystal Structure

The crystal structure of $MgMoO_4 \cdot H_2O$ and $MgWO_4 \cdot H_2O$ corresponds in its overall topology well to the model suggested in (*1*) for $MgWO_4 \cdot H_2O$. It consists of layers $(1\ -1\ 0)_{tric}$, built by edge sharing pairs of $MgO_5(H_2O)$ octahedra, which are linked by $WO_4(MoO_4)$ tetrahedra in such a way that one corner of the tetrahedron coordinates to two magnesiums and two corners to one magnesium within the planes, the fourth corner cross links these layers in the third dimension (see Fig. 1). There is one notable difference to the model structure proposed in (*1*), in that the model assumed the same orientation of the tetrahedra as in $MgWO_4 \cdot 2H_2O$, i.e., with all corners of the tetrahedra laying along rows parallel to [001] pointing in the same direction, with alternating rows pointing up and down (cf. Fig. 2 in (*1*)). The present crystal structure determi-

TABLE II

Atomic parameters for $MgMoO_4 \cdot H_2O$

Atom	x	y	z	U_{eq}[a]
Mo	0.25802(4)	0.12151(4)	0.25128(3)	0.007
Mg	0.3594(1)	0.2926(1)	−0.1944(1)	0.009
O(1)	0.3744(3)	0.3625(3)	0.1229(2)	0.010
O(2)	0.3640(3)	−0.1288(3)	0.1674(2)	0.016
O(3)	0.3653(4)	0.2341(3)	0.5050(2)	0.019
O(4)	−0.0715(3)	0.0239(3)	0.2123(3)	0.015
OW	0.0969(3)	0.4764(3)	−0.2215(3)	0.024
HW(1)	0.1237	0.6493	−0.1984	0.060
HW(2)	−0.0404	0.4229	−0.1815	0.060

Anisotropic temperature factors[b]

Atom	U_{11}	U_{22}	U_{33}	U_{23}	U_{13}	U_{12}
Mo	0.00602(7)	0.00534(7)	0.00585(7)	0.00219(5)	0.00183(5)	0.00092(5)
Mg	0.0081(3)	0.0073(3)	0.0070(3)	0.0018(2)	0.0015(2)	0.0015(2)
O(1)	0.0115(7)	0.0068(6)	0.0084(6)	0.0034(5)	0.0022(5)	−0.0006(5)
O(2)	0.0131(7)	0.0113(7)	0.0166(8)	0.0032(6)	0.0029(6)	0.0072(6)
O(3)	0.0232(9)	0.0179(8)	0.0078(7)	0.0030(6)	0.0015(6)	0.0037(7)
O(4)	0.0078(6)	0.0119(7)	0.0195(9)	0.0055(6)	0.0038(6)	0.0014(5)
OW	0.0146(8)	0.0152(9)	0.033(1)	0.0082(8)	0.0056(8)	0.0074(7)

[a] $U_{eq} = \frac{1}{3} \Sigma_i \Sigma_j U_{ij} a_i^* a_j^* a_i a_j$.

[b] The U_{ij} are defined by $\exp[-2\pi^2(U_{11}a^{*2}h^2 + U_{22}b^{*2}k^2 + U_{33}c^{*2}l^2 + 2U_{23}b^*c^*kl + 2U_{13}a^*c^*hl + 2U_{12}a^*b^*hk)]$.

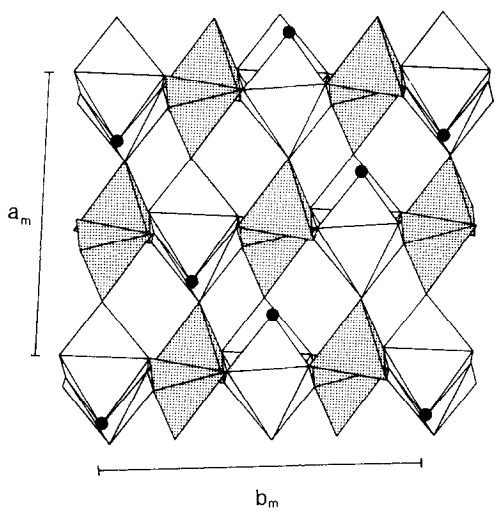

FIG. 1. View $(1\ 1\ 1)_{triclinic}$ (equivalent to $(0\ 0\ 1)_{monoclinic}$) of the crystal structure of $MgMoO_4 \cdot H_2O$, to be compared with Fig. 3b in (*1*). (Drawn with STRUPLO (*7*)). Black dots: H_2O molecules. MoO_4-tetrahedra shaded. Axes indicated belong, for ease of comparison, to the monoclinic unit cell. a_{mono} corresponds to $(a_{tric} - b_{tric})$, b_{mono} to $(a_{tric} + b_{tric} - c_{tric})$.

nation shows that in reality, at least for the crystals prepared directly as $MgMoO_4 \cdot H_2O$, the tetrahedra within one and the same row point alternatingly up and down (Fig. 1). The need for such a reorientation of the tetrahedra is the most probable cause for the high disorder (low degree of crystallinity) and intense twinning of the $MgWO_4 \cdot H_2O$ prepared by dehydration of $MgWO_4 \cdot 2H_2O$ (alternatively, it might be argued that the dehydrated material may differ in its structure from the prepared crystals, which may not be completely ruled out in view of the diffuseness of its powder X-ray diffraction pattern which prevents an accurate comparison of intensities).

Thermal Dehydration

The thermal dehydration behavior of $MgWO_4 \cdot H_2O$ essentially corresponds to that described in (*1*), with the difference

TABLE III

Interatomic distances and angles for $MgMoO_4 \cdot H_2O$

Atoms	Distance (Å)	Atoms	Distance (Å)	Atoms	Distance (Å)
Mg–O(1)	2.130(2)	Mo–O(1)	1.802(2)	OW–HW(1)	0.961(2)
Mg–O(1)′	2.088(2)	Mo–O(2)	1.757(2)	OW–HW(2)	0.842(2)
Mg–O(2)′	2.069(3)	Mo–O(3)	1.730(2)		
Mg–O(3)′	2.034(2)	Mo–O(4)	1.768(2)	Mg–Mg′	3.191(2)
Mg–O(4)′	2.066(2)			Mg–Mo	3.441(1)
Mg–OW	2.084(3)			Mo–Mo′	4.061(1)

Atoms	Angle (°)	Atoms	Angle (°)
O(1)–Mg–O(1)′	81.69(8)	O(2)′–Mg–OW	176.66(9)
O(1)–Mg–O(2)′	89.19(9)	O(3)′–Mg–O(4)′	94.50(9)
O(1)–Mg–O(3)′	176.93(9)	O(3)′–Mg–OW	90.7(1)
O(1)–Mg–O(4)′	88.02(8)	O(4)′–Mg–OW	88.95(9)
O(1)–Mg–OW	91.1(1)	O(1)–Mo–O(2)	111.19(9)
O(1)′–Mg–O(2)′	90.72(8)	O(1)–Mo–O(3)	108.31(9)
O(1)′–Mg–O(3)′	95.95(8)	O(1)–Mo–O(4)	110.1(1)
O(1)′–Mg–O(4)′	168.45(9)	O(2)–Mo–O(3)	108.7(1)
O(1)′–Mg–OW	86.03(9)	O(2)–Mo–O(4)	109.25(9)
O(2)′–Mg–O(3)′	88.9(1)	O(3)–Mo–O(4)	109.2(1)
O(2)′–Mg–O(4)′	94.39(9)	HW(1)–OW–HW(2)	103.5(3)

Hydrogen bonded contacts (Calculated with ORFFE3 (*6*))

X–H · · · Y	H · · · Y (Å)	X · · · Y (Å)	X–H · · · Y (°)
OW–HW(1) · · · O(4)″	2.038(2)	2.962(3)	161.0(1)
OW–HW(2) · · · O(2)	2.152(2)	2.920(3)	151.4(2)

Atom	Symmetry code	Atom	Symmetry code	Atom	Symmetry code
Mo	x,y,z	O(2)	x,y,z	O(4)′	$-x,-y,-z$
Mo′	$-x,-y,-z$	O(2)′	$1-x,-y,-z$	O(4)″	$-x,1-y,-z$
Mg	x,y,z	O(3)	x,y,z	OW	x,y,z
Mg′	$1-x,1-y,-z$	O(3)′	$x,y,-1+z$	HW(1)	x,y,z
O(1)	x,y,z	O(4)	x,y,z	HW(2)	x,y,z
O(1)′	$1-x,1-y,-z$				

that the anhydrous product, which corresponds to literature data for a "high temperature" modification (*8*), yields much clearer X-ray powder and pseudo-single-crystal diffraction patterns, when prepared from the monohydrate instead of the dihydrate, because its immediate precursor is obviously single crystalline and not severely twinned as when starting from the dihydrate. It now seems feasible to interpret the topotactic reaction from $MgWO_4 \cdot H_2O$ to "high temperature" $MgWO_4$ and to deduce a crystal structure model for this phase too (*9*). A high resolution electron microscopic study of this material is in progress.

In the case of $MgMoO_4 \cdot H_2O$, dehydration first leads at 190°C to a poorly crystalline material, which corresponds already roughly to the known structure of $MgMoO_4$ and recrystallizes to this phase in well-crystallized form above 600°C.

Luminescence Properties

We have recently reported the luminescence of magnesium tungstate dihydrate, $MgWO_4 \cdot 2H_2O$ (*10*). In view of the structural results on the monohydrates $MgWO_4 \cdot H_2O$ and $MgMoO_4 \cdot H_2O$, it seemed interesting to investigate also the luminescence of these two compounds and to compare the results for the dihydrates, the monohydrates, and the anhydrous compounds.

The optical instrumentation used is the same as mentioned in (*10*), and consists essentially of a Perkin-Elmer spectrofluorometer MPF-3 equipped with a Xe lamp and a helium cryostat. The spectral data obtained are very similar to those reported for $MgWO_4 \cdot 2H_2O$ as far as band shape is concerned.

$MgWO_4 \cdot 2H_2O$ shows two different emissions which are independent of each other, viz., a blue emission which is related to the presence of water, and a greenish emission from the tungstate tetrahedron. The latter is due to a charge transfer transition in the tungstate group. None of the other samples shows the blue emission, whatever the temperature or excitation wavelength may be. This seems to indicate that the blue emission is not due to intrinsic water molecules, but rather to water (or hydroxide groups) on the surface (see Ref. (*10*) and references cited herein).

All molybdate and tungstate samples show broadband excitation spectra like those reported for the tungstate luminescence of $MgWO_4 \cdot 2H_2O$ (*10*). No luminescence was observed for $MgMoO_4 \cdot 2H_2O$, not even at 4.2 K. According to the literature, water-free $MgMoO_4$ does not luminesce at 77 K (*11*). We prepared $MgMoO_4$ as described in (*11*) and observed at 4.2 K an orange emission, which persists up to 250 K. In Table IV we have compiled our results by presenting the maxima of the emission bands, the maxima of the excitation bands, the Stokes shifts of the emissions, and the thermal quenching temperatures of the emissions of the compounds under investigation. For those that do not luminesce, the position of the optical band edge estimated from the reflectance spectrum is given. This value can be compared with the position of the excitation maxi-

TABLE IV

LUMINESCENCE PROPERTIES OF SEVERAL MOLYBDATES AND TUNGSTATES

Compound	Emission maximum (nm)	Excitation maximum (nm)	Stokes shift (10^3 cm^{-1})	Quenching temp. (K)	Ref.
$MgWO_4 \cdot 2H_2O$	480	270	17	200	(*10*)
$MgWO_4 \cdot H_2O$	465	250	19	300	*
$MgWO_4$ (wolframite)	470	295	13.5	450	(*10*)
$SrWO_4$ (scheelite)	460	245	19.5	300	(*10*)
$MgMoO_4 \cdot 2H_2O$	—	320[a]	—	—	*
$MgMoO_4 \cdot H_2O$	540	270	19	150	*
$MgMoO_4$ (α-$MnMoO_4$)[b]	~520 ~620	~275 ~310	~17	~250	*
$Mg(W,Mo)O_4$ (wolframite)	680	360	13.5	—	(*11*)
$SrMoO_4$ (scheelite)	530	280	17.5	200	(*12*)

* This work.

[a] No luminescence, see text.

[b] There is a weak additional emission with a maximum at ~700 nm and an excitation maximum at ~340 nm.

mum, since the excitation and absorption bands correspond to the same electronic transition, viz., the charge-transfer transition of the molybdate group. The previous results and some literature data are added to this table. According to spectral analysis, the monohydrates are contaminated by a few percent of dihydrate. Our optical measurements are more sensitive in this aspect than X-ray powder diffraction analysis.

The luminescence properties of $MgWO_4 \cdot H_2O$ are different from those of $MgWO_4 \cdot 2H_2O$. In the monohydrate the spectral bands are at higher energy and the quenching temperature is higher. The properties of $MgWO_4 \cdot H_2O$ are very similar to those of the scheelite $SrWO_4$.

In (*10*) it was argued that the low-energy position of the spectral band of $MgWO_4 \cdot 2H_2O$ (which implies a low quenching temperature) is due to the unsaturated character of O(3). This in turn is a consequence of the layer structure of $MgWO_4 \cdot 2H_2O$, the O(3) ion being an oxygen ion which is only bonded to tungsten and not to magnesium. The crystal structure of $MgWO_4 \cdot H_2O$ is different, because every oxygen ion is bonded to tungsten as well as to magnesium. This results from the fact that the layer character of the dihydrate structure is lost in the monohydrate. It is satisfying to note that the spectra of the monohydrate move to higher energy and become similar to those for a compound with a three-dimensional lattice like $SrWO_4$.

It is well known that the molybdate group has its spectral features at considerably lower energy than the tungstate group and that the molybdate luminescence has, consequently, a lower quenching temperature (*12, 13*). This can also be observed in Table IV. The luminescence of $MgMoO_4 \cdot H_2O$, which is similar to that of $SrMoO_4$, is at lower energy and has a lower quenching temperature that that of the isomorphous $MgWO_4 \cdot H_2O$.

The dihydrates have very similar crystal structures (*1, 14*), although their symmetry is slightly different. For our present purposes we can neglect this small difference. This means that we are able to estimate the emission maximum of $MgMoO_4 \cdot 2H_2O$ by using the data of $MgWO_4 \cdot 2H_2O$ and the value of the optical band edge of the molybdate. This yields an emission maximum of about 700 nm. Obviously the nonradiative rate exceeds the radiative rate considerably, because no luminescence could be observed.

A comparison with the water-free compounds is difficult. In $MgWO_4$ (wolframite), the tungsten coordination is octahedral instead of tetrahedral. The charge-transfer absorption moves to lower energy with an increasing number of coordinating ligands (see Table IV) and the Stokes shift decreases (*9*). In fact, $MgWO_4$ is a commercially applied luminescent material. A comparison with $MgMoO_4$ makes no sense, since $MgMoO_4$ has the α-$MnMoO_4$ structure with tetrahedral MoO_4-groups (*15, 16*). Kröger (11) has reported the luminescence of the molybdate group diluted in the wolframites $MgWO_4$ and $ZnWO_4$ (see Table IV). His data show in comparison to those of $MgWO_4$ the trends indicated above.

The data illustrate also that the thermal quenching temperature of broadband luminescence decreases if the energy levels shift to low energy and if the Stokes shift is large. This is a direct consequence of the configurational coordinate diagram (*17*).

Finally we consider $MgMoO_4$, which has a rather complicated crystal structure (*15, 16*). The two emission bands with the corresponding excitation spectra are assigned to the two crystallographically different molybdate groups in the crystal structure (*15*). It is impossible to separate these two emissions spectrally which makes the data in Table IV rather inaccurate. The additional emission (see Table IV) is ascribed to a defect molybdate group, following similar ob-

servations for $CaMoO_4$ (*18*). It is satisfying to note that the averaged values for the molybdate luminescence of $MgMoO_4$ are about equal to those for $MgMoO_4 \cdot H_2O$ and $SrMoO_4$, as is to be expected from the structural analogy (three-dimensional molybdate lattice).

Acknowledgments

The authors are indebted to Mrs. G. J. Dirksen and R. C. A. Keller for their assistance in the optical measurements.

References

1. J. R. GÜNTER AND E. DUBLER, *J. Solid State Chem.* **65,** 118 (1986).
2. M. AMBERG, Diploma thesis, University of Zurich (1988).
3. J. R. GÜNTER, AND X.-L. XU, unpublished results.
4. G. M. SHELDRICK, SHELX76, Program for Crystal Structure Determination, University of Cambridge, England (1976).
5. G. M. SHELDRICK, SHELXS86, *in* "Crystallographic Computing" (G. M. Sheldrick, C. Krüger, and R. Goddard, Eds.), pp. 175–189, Oxford Univ. Press, London/New York (1985).
6. W. R. BUSING, K. O. MARTIN, H. A. LEVY, G. M. BROWN, C. K. JOHNSON, AND W. A. THIESSEN, ORFFE3, A Fortran Function and Error Program, Oak Ridge National Lab., TN (1971).
7. R. X. FISCHER, STRUPLO, *J. Appl. Crystallogr. Sect. B* **32,** 1957 (1976).
8. L. L. Y. CHANG, M. G. SCROGER, AND B. PHILLIPS, *J. Amer. Ceram. Soc.* **49,** 385 (1966).
9. J. R. GÜNTER AND M. AMBERG, "Proc. 11th Int. Symp. on the Reactivity of Solids, Princeton, 1988." *Solid State Ionics,* in press.
10. G. BLASSE, G. J. DIRKSEN, M. HAZENKAMP, AND J. R. GÜNTER, *Mat. Res. Bull.* **22,** 813 (1987); due to retyping in the editorial office this paper contains some serious misprints, which are corrected in the present contribution.
11. F. A. KRÖGER, *Philips Res. Repts.* **2,** 177 (1947).
12. F. A. KRÖGER, "Some Aspects of the Luminescence of Solids," Elsevier, Amsterdam (1948).
13. G. BLASSE, *Struct. Bonding* **42,** 1 (1980).
14. J. Y. LE MAROUILLE, O. BARS, AND D. GRANDJEAN, *Acta Crystallogr. Sect. B* **36,** 2558 (1980).
15. S. C. ABRAHAMS AND J. M. REDDY, *J. Chem. Phys.* **43,** 2533 (1965).
16. G. W. SMITH, *Acta Crystallogr.* **15,** 1054 (1962); A. W. SLEIGHT AND B. L. CHAMBERLAND, *Inorg. Chem.* **7,** 1672 (1968).
17. G. BLASSE, *Mat. Chem. Phys.* **16,** 201 (1987).
18. J. A. GROENINK, C. HAKFOORT, AND G. BLASSE, *Phys. Stat. Sol. (a)* **54,** 477 (1979).